**Figure 4.29:** Covered conveyor belt for limestone transport (Copyright Halliburton Energy Services).

**Figure 4.30:** Exterior view of dome storage unit with conveyor loading port (Copyright Halliburton Energy Services).

The dome storage unit has a capacity of 60 kilotons, and is filled by dispensing the rock from the conveyor at the top of the dome into a pile built in a circular pattern (Figure 4.31). The rock is reclaimed from storage via a raking device (Figure 4.32) that grates over the pile at the natural angle of material slide. The raked material slides to the base of the raking unit, where a second conveyor system transfers material to either of two limestone buffer bins (Figure 4.33), each of which is dedicated to a particular kiln process. There is an additional buffer bin for mill scale from a nearby steel plant, as well as a buffer bin for sand. It is worth noting at this point that the mill scale from the steel plant contains significant levels of boron, which acts as an innate retarder and seems to affect adversely, though not overly severely, the early compressive strength development when compared to cement from other plants.

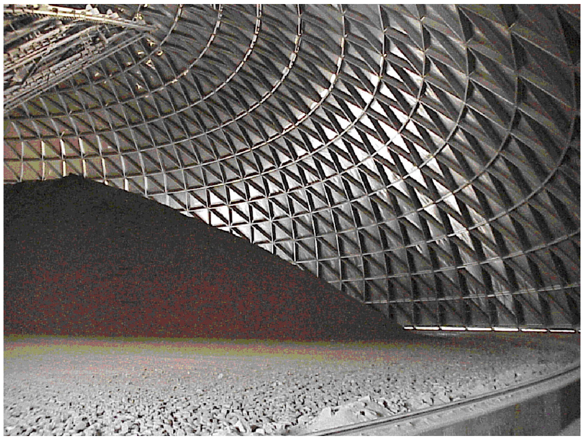

**Figure 4.31:** Interior view of dome storage unit, illustrating its radial piling (Copyright Halliburton Energy Services).

**Figure 4.32:** Raking device for reclaiming stored limestone (Copyright Halliburton Energy Services).

**Figure 4.33:** Buffer bin (Copyright Halliburton Energy Services).

Material leaving the buffer bins is monitored for elemental composition via XRF and feed rates are adjusted for maintaining proper flow of calcium, silicon, aluminum, and iron. The raw materials are carried to ball mills (Figure 4.34) for grinding to fine powder, which is then mixed with water. The resulting slurry is then sent to the rotary kiln for burning (Figure 4.35), or transformation into cement clinker.

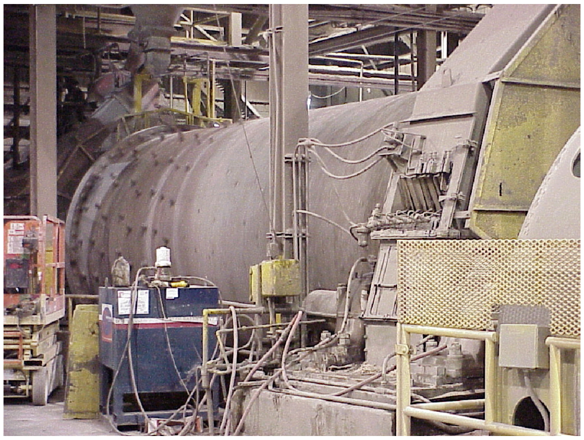

**Figure 4.34:** Coarse grinder (Copyright Halliburton Energy Services).

**Figure 4.35:** A wet rotary kiln (Copyright Halliburton Energy Services).

The kilns are fired to an internal material temperature of 2700 °F (Figure 4.36) with a fuel of finely ground coal, natural gas, and/or various waste materials. Around fifty percent of the energy expenditure in the wet kiln process is dedicated to evaporating the water from the slurry, in contrast to the dry process, which spends most of its energy on the calcining process. Since the dry process only requires approximately half the energy of the wet process, it is generally more attractive to cement manufacturers. Unfortunately, the dry process in current use produces poor API Class H cement. A fuller understanding of the differences in cement synthesis via the two processes could lead to the development of a more effective dry synthesis of Class H cements, but that is beyond the scope of this work.

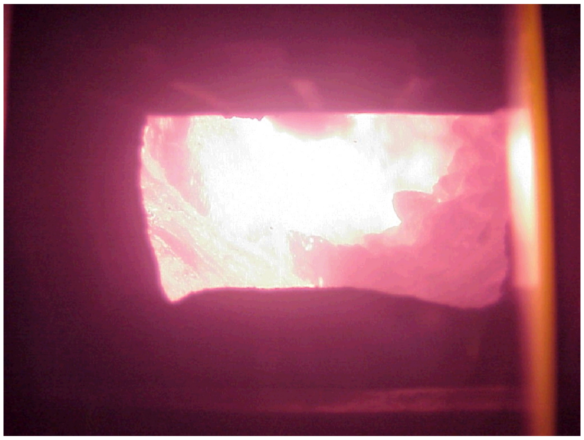

**Figure 4.36:** Interior view of an operational wet kiln (Copyright Halliburton Energy Services).

After the clinker leaves the kiln, it enters a cooler that uses pressurized air to cool the clinker. The energy absorbed by the air in the cooler serves to pre-heat the air for feed into the kiln. The cooled clinker is then taken to storage to await final grinding with approximately five percent gypsum by weight. After grinding to the specified fineness, the final cement powder is pneumatically transferred to storage silos until it is shipped to the customer.

Quality control of the clinker and final powder is handled via an automated X-ray diffraction/X-ray fluorescence (XRD/XRF) system, simple wet chemical analyses, simple optical microscopy, and periodic performance tests, including compressive strength and thickening time. This entire process results in the heterogeneous nanocomposite of calcium silicate and aluminate particles, among other materials, which make up a typical cement grain.

### 4.2.3.3 Hydration of Portland Cement[6]

#### 4.2.3.3.1

The addition of water to dry cement powder results in a thin cement slurry that can be easily manipulated and cast into different shapes. In time, the slurry sets and develops strength through a series of hydration reactions. Hydration of cement is not linear through time, it proceeds very slowly at first, allowing the thin mixture to be properly placed before hardening. The chemical reactions that cause the delay in hardening are not completely understood; however, they are critical to developing a rational methodology for the control of cement setting.

##### 4.2.3.3.1.1 Tri- and di-calcium silicates

The tri- and di-calcium silicates (C3S and C2S, respectively) comprise over 80% by weight of most cement. It is known that C3S is the most important phase in cement for strength development during the first month, while C2S reacts much more slowly, and contributes to the long-term strength of the cement. Both the silicate phases react with water as shown below to form calcium hydroxide and a rigid calcium-silicate hydrate gel, C–S–H, (4.19) and (4.20).

$$2\,(CaO)_3(SiO_2) + 7\,H_2O \rightarrow (CaO)_3(SiO_2)_2 \cdot 4(H_2O) + 3\,Ca(OH)_2 \tag{4.19}$$

$$2\,(CaO)_2(SiO_2) + 5\,H_2O \rightarrow (CaO)_3(SiO_2)_2 \cdot 4(H_2O) + Ca(OH)_2 \tag{4.20}$$

The detailed structure of C–S–H is not completely known, however it is generally agreed upon that it consists of condensed silicate tetrahedra sharing oxygen atoms with a central, calcium hydroxide-like $CaO_2$ layer. Calcium hydroxide consists of hexagonal layers of octahedrally coordinated calcium atoms and tetrahedrally coordinated oxygen atoms. Taylor has proposed that the structure is most similar to either Tobermorite or Jennite, both of which share a skeletal silicate chain Figure 4.37.

---

[6] This content is available online at <http://cnx.org/content/m16447/1.11/>.

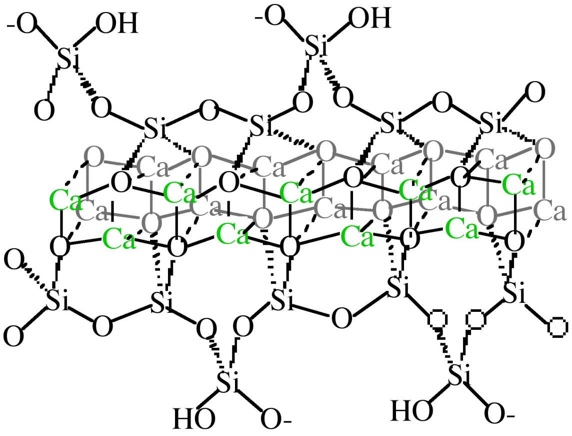

**Figure 4.37:** Schematic representation of Tobermorite, viewed along a polysilicate chain. Silicate ions either share oxygen atoms with a central $CaO_2$ core or bridge silicate tetrahedra. Interlayer calcium ions and water molecules are omitted for clarity.

Although the precise mechanism of C3S hydration is unclear, the kinetics of hydration is well known. The hydration of the calcium silicates proceeds via four distinct phases as shown in Figure 4.38. The first 15-20 minutes, termed the pre-induction period (Figure 4.38a), is marked by rapid heat evolution. During this period calcium and hydroxyl ions are released into the solution. The next, and perhaps most important, phase is the induction period (Figure 4.38b), which is characterized by very slow reactivity. During this phase, calcium oxide continues to dissolve producing a pH near 12.5. The chemical reactions that cause the induction period are not precisely known; however, it is clear that some form of an activation barrier must be overcome before hydration can continue. It has been suggested that in pure C3S, the induction period may be the length of time it takes for C–S–H to begin nucleation, which may be linked to the amount of time required for calcium ions to become supersaturated in solution. Alternatively, the induction period may be caused by the development of a small amount of an impermeable calcium-silicon-hydrate (C–S–H) gel at the surface of the particles, which slows down the migration of water to the inorganic oxides. The initial Ca/Si ratio at the surface of the particles is near 3. As calcium ions dissolve out of this C–S–H gel, the Ca/Si ratio in the gel becomes 0.8-1.5. This change in Ca/Si ratio corresponds to a change in gel permeability, and may indicate an entirely new mechanism for C–S–H formation. As the initial C–S–H gel is transformed into the more permeable layer, hydration continues and the induction period gives way to the third phase of hydration, the acceleratory period (Figure 4.38c).

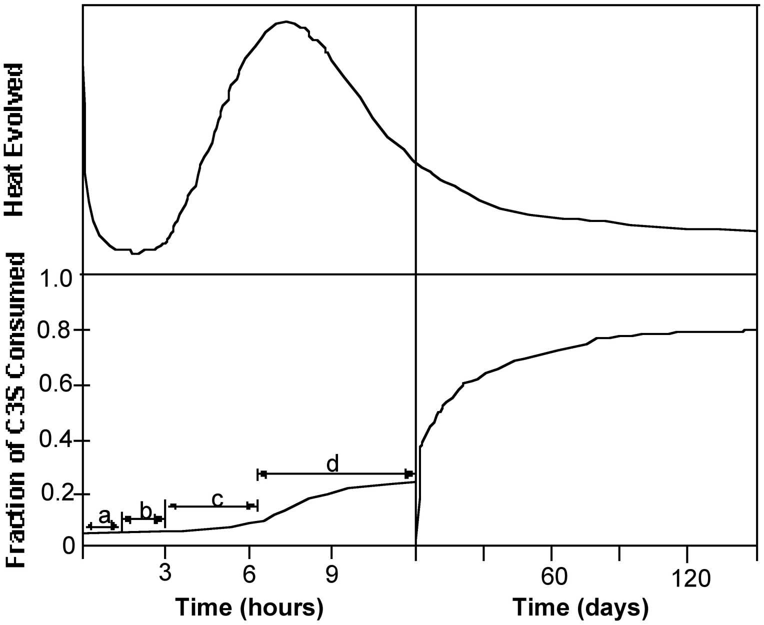

**Figure 4.38:** Hydration of C3S over time: (a) the preinduction period, (b) the induction, (c) period the acceleratory period, and (d) the deceleratory period.

After ca. 3 hours of hydration, the rate of C–S–H formation increases with the amount of C–S–H formed. Solidification of the paste, called setting, occurs near the end of the third period. The fourth stage (Figure 4.38d) is the deceleratory period in which hydration slowly continues hardening the solid cement until the reaction is complete. The rate of hydration in this phase is determined either by the slow migration of water through C–S–H to the inner, unhydrated regions of the particles, or by the migration of $H^+$ through the C–S–H to the anhydrous CaO and $SiO_2$, and the migration of $Ca^{2+}$ and $Si^{4+}$ to the $OH^-$ ions left in solution.

#### 4.2.3.3.1.2 Calcium aluminate and ferrite

In spite of the fact that the aluminate and ferrite phases comprise less than 20% of the bulk of cement, their reactions are very important in cement and dramatically affect the hydration of the calcium silicate phases, see below. Relative to C3S, the hydration of C3A is very fast. In the absence of any additives, C3A reacts with water to form two intermediate hexagonal phases, C2AH8 and C4AH13, (4.21). The structure of C2AH8 is not precisely known, but C4AH13 has a layered structure based on the calcium hydroxide structure, in which one out of every three $Ca^{2+}$ is replaced by either an $Al^{3+}$ or $Fe^{3+}$ with an $OH^-$ anion in the interlayer space to balance the charge. All of the aluminum in C4AH13 is octahedral. C2AH8 and C4AH13 are meta-stable phases that spontaneously transform into the fully hydrated, thermodynamically stable cubic phase, C3AH6, (4.22). In C3A, aluminum coordination is tetrahedral. The structure consists of rings of aluminum tetrahedra linked through bridging oxygen atoms, which slightly distorts the aluminum environment. In C3AH6, aluminum exists as highly symmetrical, octahedral $Al(OH)_6$ units.

$$2\,(CaO)_3(Al_2O_3) + 21\,H_2O \rightarrow (CaO)_4(Al_2O_3)\cdot 13(H_2O) + (CaO)_2(Al_2O_3)\cdot 8(H_2O) \qquad (4.21)$$

$$(CaO)_4(Al_2O_3)\cdot 13(H_2O) + (CaO)_2(Al_2O_3)\cdot 8(H_2O) \rightarrow 2\ (CaO)_3(Al_2O_3)\cdot 6(H_2O) + 9\ H_2O \tag{4.22}$$

If the very rapid and exothermic hydration of C3A is allowed to proceed unhindered in cement, then the setting occurs too quickly and the cement does not develop strength. Therefore, gypsum [calcium sulfate dihydrate, $CaSO_4\cdot 2(H_2O)$] is added to slow down the C3A hydration. In the presence of gypsum, tricalcium aluminate forms ettringite, $[Ca_3Al(OH)_6.12(H_2O)]_2.(SO_4)_3.2(H_2O)$, (4.23), which can also be written as $C3A.3(CaSO_4).32(H_2O)$. Ettringite grows as columns of calcium, aluminum and oxygen surrounded by water and sulfate ions, as shown in Figure 4.39.

$$(CaO)_3(Al_2O_3) + 3\ CaSO_4\cdot 2(H_2O) + 26\ H_2O \rightarrow (CaO)_3(Al_2O_3)(CaSO_4)_3\cdot 32(H_2O) \tag{4.23}$$

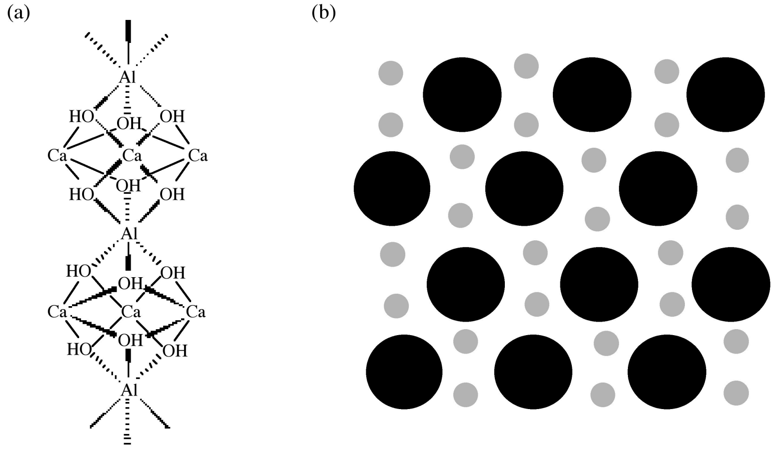

**Figure 4.39:** Ettringite columns (a) consisting of octahedral aluminum, tetrahedral oxygen, and 8-coordinate calcium. The coordination sphere of each calcium is filled by water and sulfate ions. The packing of the columns (b) represented by large circles, the smaller circles represent channels containing with water and sulfate ions.

Tetracalcium aluminoferrite (C4AF) reacts much like C3A, i.e., forming ettringite in the presence of gypsum. However, hydration the ferrite phase is much slower than hydration of C3A, and water is observed to bead up on the surface of C4AF particles. This may be due to the fact that iron is not as free to migrate in the pastes as aluminum, which may cause the formation of a less permeable iron rich layer at the surface of the C4AF particles and isolated regions of iron hydroxide. In cement, if there is insufficient gypsum to convert all of the C4AF to ettringite, then an iron-rich gel forms at the surface of the silicate particles which is proposed to slow down their hydration.

#### 4.2.3.3.1.3 Portland cement

The hydration of cement is obviously far more complex than the sum of the hydration reactions of the individual minerals. The typical depiction of a cement grain involves larger silicate particles surrounded by the much smaller C3A and C4AF particles. The setting (hydration) of cement can be broken down into several distinct periods. The more reactive aluminate and ferrite phases react first, and these reactions dramatically affect the hydration of the silicate phase. Scrivener and Pratt used TEM to develop the widely accepted model depicted in Figure 4.40.

In the first few minutes of hydration (Figure 4.40b), the aluminum and iron phases react with gypsum to form an amorphous gel at the surface of the cement grains and short rods of ettringite grow. After this initial period of reactivity, cement hydration slows down and the induction period begins. After about 3 hours of hydration, the induction period ends and the acceleratory period begins. During the period from 3 to 24 hours, about 30% of cement reacts to form calcium hydroxide and C–S–H. The development of C–S–H in this period occurs in 2 phases. After ca. 10 hours hydration (Figure 4.40c), C3S has produced "outer C–S–H," which grows out from the ettringite rods rather than directly out from the surface of the C3S particles. Therefore, in the initial phase of the reaction, the silicate ions must migrate through the aluminum and iron rich phase to form the C–S–H. In the latter part of the acceleratory period, after 18 hours of hydration, C3A continues to react with gypsum, forming longer ettringite rods (Figure 4.40d). This network of ettringite and C–S–H appears to form a "hydrating shell" about 1 $\mu$m from the surface of anhydrous C3S. A small amount of "inner C–S–H" forms inside this shell. After 1–3 days of hydration, reactions slow down and the deceleratory period begins (Figure 4.40e). C3A reacts with ettringite to form some monosulfate. "Inner C–S–H" continues to grow near the C3S surface, narrowing the 1 $\mu$m gap between the "hydrating shell" and anhydrous C3S. The rate of hydration is likely to depend on the diffusion rate of water or ions to the anhydrous surface. After 2 weeks hydration (Figure 4.40f), the gap between the "hydrating shell" and the grain is completely filled with C–S–H. The original, "outer C–S–H" becomes more fibrous.

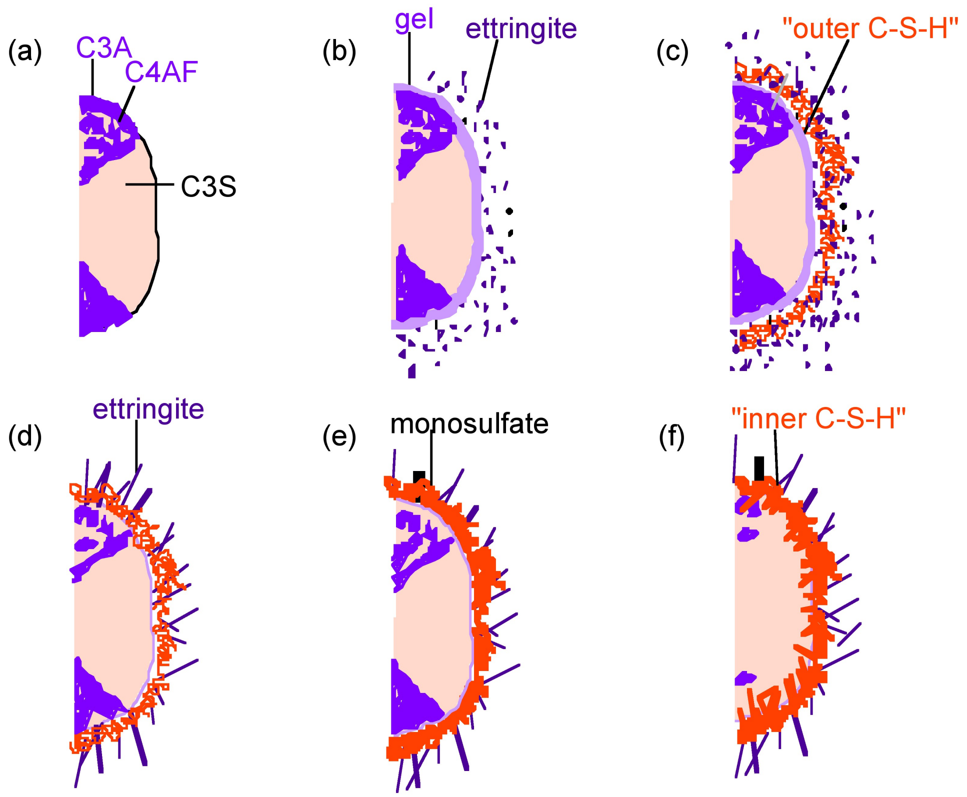

**Figure 4.40:** Schematic representation of anhydrous cement (a) and the effect of hydration after (b) 10 minutes, (c) 10 hours, (d) 18 hours, (e) 1–3 days, and (f) 2 weeks. Adapted from M. Bishop, PhD Thesis, Rice University, 2001.

#### 4.2.3.3.2 Bibliography

- H. F. W. Taylor, *Cement Chemistry*, 2nd Ed., Academic Press, London (1997).
- H. F. W. Taylor, *J. Am. Ceram. Soc.*, 1986, **69**, 464.
- V. S. Ramanchandran, R.F. Feldman, and J. J. Beaudoin, *Concrete Science*, Heyden and Son Ltd., Philadelphia, PA, 1981.
- H. N. Stein and J. Stevels, *J. App. Chem.*, 1964, **14**, 338.
- M. Grutzeck, S. Kwan, J. Thompson, and A. Benesi, *J. Mater. Sci. Lett.*, 1999, **18**, 217.
- V. S. Ramachandran, *Concrete Admixtures Handbook*, 2nd Edition, Noyes Publications, New Jersey (1995).
- K. L. Scrivener and P. L. Pratt, *Mater. Res. Soc. Symp. Proc.*, 1984, **31**, 351.

### 4.2.3.4 Hydration Inhibition of Portland Cement[7]

#### 4.2.3.4.1

In the oil industry, Portland cement supports boreholes of ever increasing depth. This application requires a high degree of control over the setting kinetics to allow the cement to be pumped down in a liquid form. A number of chemical inhibitors are employed to delay the setting time. The ideal inhibitor for oil well cementing would predictably delay the setting of cement, and then suddenly allow hydration to continue at a rapid rate.

A wide range of compounds show set inhibition of the hydration of Portland cement. Some common examples include, sucrose, tartaric acid, gluconic acid $\delta$-lactone, lignosulfonate, and organic phosphonic acids, in particular nitrilo-tris(methylene)phosphonic acid ($H_6$ntmp). The structures of these retarders are shown in .

---

[7] This content is available online at <http://cnx.org/content/m16446/1.12/>.

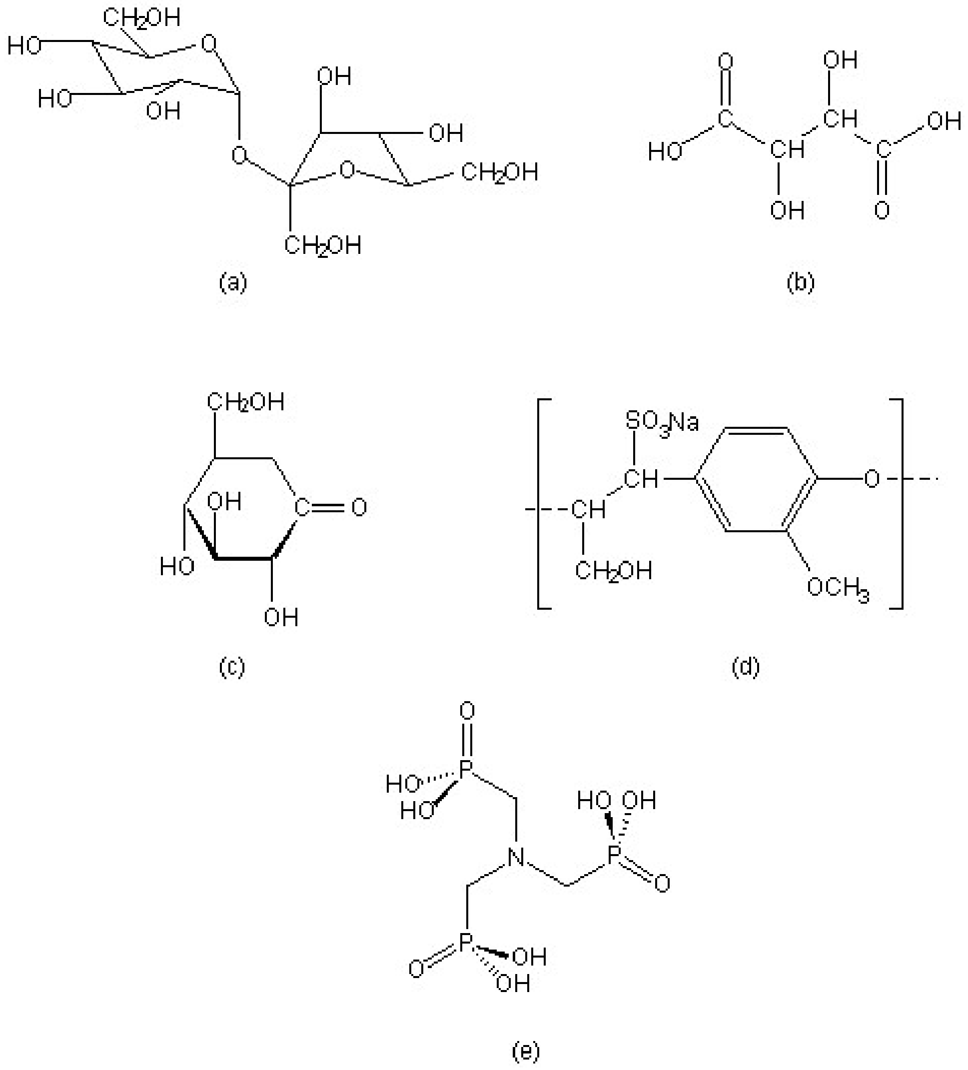

**Figure 4.41:** Structural formulae of common cement retarders. (a) sucrose, (b) tartaric acid, (c) gluconic acid d-lactone, (d) sodium lignosulfonate, and (e) nitrilo-tris(methylene)phosphonic acid ($H_6$ntmp).

In spite of the fact that the science of cement hydration inhibition has been investigated for over 40 years, the mechanistic details are still the subject of much speculation. There are five primary models for cement hydration inhibition: calcium complexation, nucleation poisoning, surface adsorption, protective coating/osmotic bursting, and dissolution-precipitation. A summary of the characteristic behavior of selected retarders is shown in Table 4.7.

| **Retarder** | **Characteristic behavior** |
|---|---|
| sucrose | Ca binding, acts directly on silicates, accelerates ettringite formation |
| tartaric acid | acts via calcium complexation and calcium tartrate coating, inhibits ettringite formation |
| lignosulfonate | accelerates ettringite formation, calcium becomes incorporated into the polymer matrix during hydration, forms a diffusion barrier |
| nitrilo-tris(methylene)phosphonic acid ($H_6$ntmp) | promotes Ca dissolution, forms [Ca($H_6$ntmp)], heterogeneous nucleation on aluminates creates a protective coating around the grain |

**Table 4.7**: Summary of the behavior of various hydration retarders.

#### 4.2.3.4.1.1 Calcium complexation

Inhibition by calcium complexation relies largely on the requirement that small calcium oxide/hydroxide templates must form in the pore water of cement pastes before silicate tetrahedra can condense into dimeric and oligomeric silicates to form C–S–H. Calcium complexation involves either removing calcium from solution by forming insoluble salts, or chelating calcium in solution. Calcium complexation lowers the amount of calcium effectively in solution, delaying the time to $Ca(OH)_2$ super-saturation and preventing precipitation of the necessary templates. Simple calcium complexation should dramatically increase the amount of $Si(OH)_4$ tetrahedra in solution, and indeed this is observed with most retarders. However, if the retarder were acting solely by calcium complexation, then one molecule of retarder would be required per calcium ion in solution, and good inhibitors are used in much smaller quantities, on the order of 0.1-2% by weight of cement. In addition, there is no simple correlation between either calcium binding strength or calcium salt solubility and retarding ability. Yet it has been shown that in pure systems, i.e., of C3S and C2S, that the lime concentration in solutions is the most important factor in determining the precipitation of C–S–H. Therefore, although calcium complexation must play some role in inhibition, other mechanisms of inhibition must be at work as well. An example of a retarder that operates primarily through calcium complexation is tartaric acid, however, the formation of insoluble calcium tartrate on cement grains suggest that dissolution/precipitation occurs in addition (Figure 4.42).

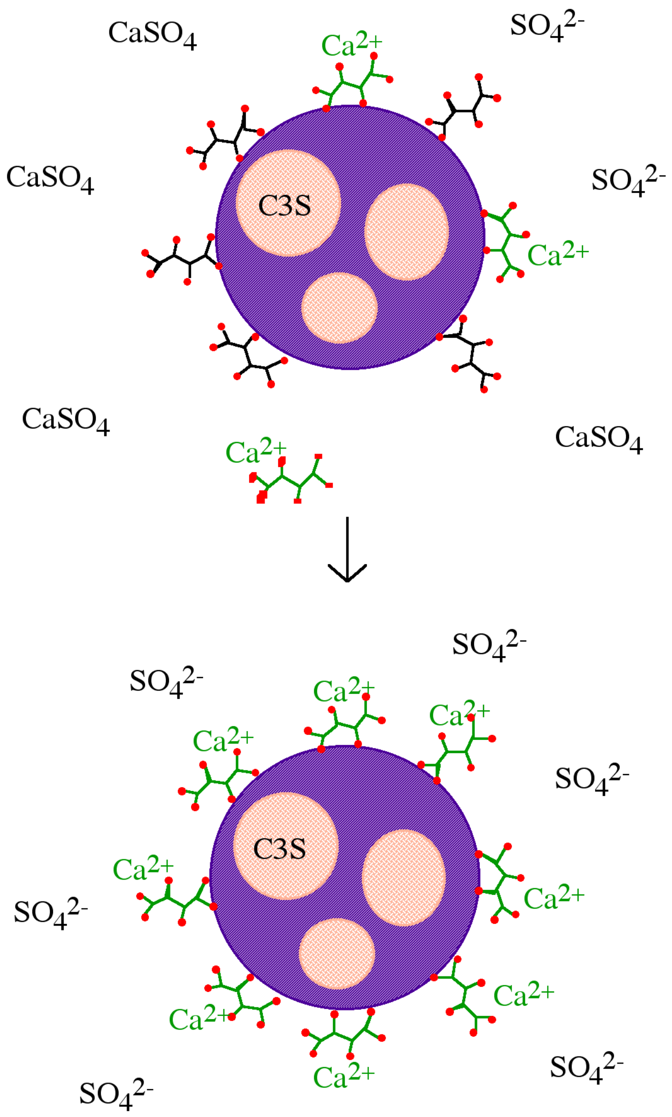

**Figure 4.42:** Schematic representation of cement hydration in the presence of tartaric acid. The aluminate (and aluminate ferrate) phases (shown in purple) surround the silicate phases (C3S and C2S). Tartaric acid adsorbs onto the aluminum surfaces and reacts with calcium ions from gypsum to deposit a thick calcium tartrate coating on the cement grain. Adapted from M. Bishop, PhD Thesis, Rice University, 2001.

#### 4.2.3.4.1.2 Nucleation poisoning

As with calcium complexation, nucleation poisoning must rely on the formation of small calcium oxide/hydroxide templates in the pore water of cement pastes before silicate tetrahedra can condense into dimeric and oligomeric silicates to form C–S–H. Inhibition by nucleation poisoning is where the retarder blocks the growth of C–S–H or $Ca(OH)_2$ crystals through inhibiting agglomerates of calcium ions from forming the necessary hexagonal pattern. Nucleation inhibitors act on the surface of small clusters, therefore, less than one molecule of retarder per calcium ion is required to produce dramatic results. This type of inhibition also results in an increase in the amount of silicate ions in solution, as condensation of silicate chains onto calcium oxide templates to form the C–S–H is inhibited. As a retarder sucrose acts via nucleation poisoning/surface adsorption.

#### 4.2.3.4.1.3 Surface adsorption

Surface adsorption of inhibitors directly onto the surface of either the anhydrous or (more likely) the partially hydrated mineral surfaces blocks future reactions with water. In addition, if such inhibitors are large and anionic, then they produce a negative charge at the surface of the cement grains, causing the grains to repel each other thereby reducing inter-particle interactions. Lignosulfonates are typical of retarders that act via surface adsorption.

#### 4.2.3.4.1.4 Protective coating/osmotic bursting

The formation of a protective coating with its subsequent bursting due to the build up of osmotic pressure was originally posited to explain the existence of the induction period in C3S and cement hydration, however it may be applied to inhibition in general. In this mechanism, a semi-permeable layer at the surface of the cement grain forms and slows down the migration of water and lengthens the induction period. Osmosis will drive water through the semi-permeable membrane towards the unhydrated mineral, and eventually the flow of water creates higher pressure inside the protective coating and the layer bursts. Hydration is then allowed to continue at a normal rate.

#### 4.2.3.4.1.5 Dissolution-precipitation

A detailed study of several retarders (in particular the organic phophonates) has shown that the actually accelerate certain stages of the hydration process. This is unexpected since the phosphonates have been termed "super retarders," due to their increased effect on cement hydration relative to the effect of conventional retarders. So how is it that a retarder can be so efficient at hydration inhibition at the same time as accelerating the process? The ability of phosphonates to retard cement setting is due to the lengthening the induction period, without slowing down the time it takes for setting to occur (once the acceleratory period has begun).

Phosphonates are known to complex calcium and other $M^{2+}$ cations, poison the nucleation and growth of barium sulfate crystals, and inhibit the hydration of $Fe_2O_3$ and $Al_2O_3$ surfaces via direct surface adsorption, thus it was assumed that with regard to cement hydration inhibition occurred by one of these mechanism. However, the mechanism by which phosphonates inhibit cement hydration consists of two steps. First dissolution, whereby calcium is extracted from the surface of the cement grains (Figure 4.43a) exposing the aluminum rich surface to enhanced (catalyzes) hydration and ettringite formation (Figure 4.43b). Second precipitation, whereby the soluble calcium-phosphonate oligomerizes either in solution or on the hydrate surface to form an insoluble polymeric Ca-phosphonate (Figure 4.43c). The Ca-phosphonate material binds to the surface of the cement grains inhibiting further hydration by acting as a diffusion barrier to water as well as a nucleation inhibitor.

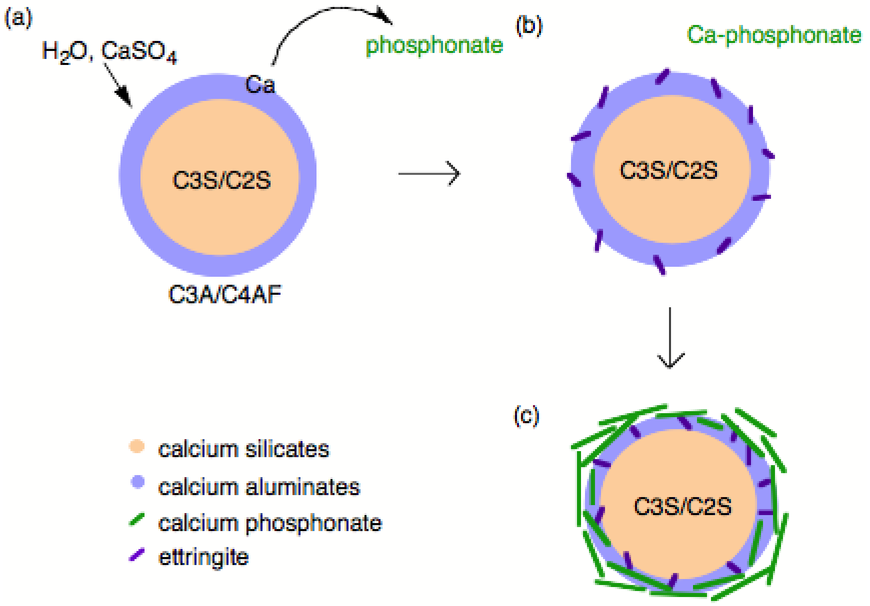

**Figure 4.43:** Schematic representation of the $H_6$ntmp inhibition of cement showing (a) the phosphonic acid promoting calcium dissolution, allowing water and gypsum to react with the aluminum phases at the surface of the cement grain, (b) the formation of a meta-stable calcium phosphonate, which precipitates onto the hydrating aluminate surfaces (c), forming a barrier to water and sulfate diffusion. Adapted from M. Bishop, PhD Thesis, Rice University, 2001.

#### 4.2.3.4.2 Bibliography

- N. Thomas and J. Birchall, *Cement and Concrete Research*, 1983, **13**, 830.
- D. Double, *Phil. Trans. R. Soc. London*, 1983, **A30**, 53.
- M. Bishop, S. G. Bott, and A. R. Barron, *Chem. Mater.*, 2003, **15**, 3074.
- M. Bishop and A. R. Barron, *Ind. Eng. Chem. Res.*, 2006, **45**, 7042.

## 4.3 Differences for Beryllium and Magnesium[8]

While the chemistry of strontium, barium (and radium) is similar to that of calcium, magnesium and beryllium show marked differences. In both cases these differences are due to the small size of the ions.

### 4.3.1 Beryllium

Beryllium can be thought of as being even more covalent than magnesium. The small size (*ca.* 0.3 Å) results in a very high charge density of $Be^{2+}$. In addition, the ionization energy for beryllium is a large positive value (1st ionization energy = 899.5 kJ/mol, 2nd ionization energy = 14,848.7 kJ/mol). Both of these factors means that the free ion does not exist. Instead, beryllium forms covalent compounds in a similar manner to

---

[8] This content is available online at <http://cnx.org/content/m31919/1.4/>.

its diagonal analog aluminum. Both beryllium and aluminum form covalent compounds or strongly solvated cations, and both form polymeric hydrides, chlorides, and alkyls.

Beryllium chloride is not a lattice structure with a concomitantly high melting and boiling point as observed for the other Group 2 metals (Table 4.8). Instead $BeCl_2$ is a polymer in the solid state (Figure 4.44a), and an equilibrium between a monomer (Figure 4.44b) and dimer (Figure 4.44c) in the vapor phase.

| M | Structure |
|---|---|
| Be | Polymer (4-coordinate Be) |
| Mg | Cadmium chloride structure (6-coordinate Mg) |
| Ca | Deformed rutile structure (6-coordinate Ca) |
| Sr | Deformed rutile structure (6-coordinate Sr) |
| Ba | $PbCl_2$ structure (9-coordinate Ba) or fluorite structure (8-coordinate Ba) |

**Table 4.8**: Summary of structures for alkaline earth chlorides ($MCl_2$).

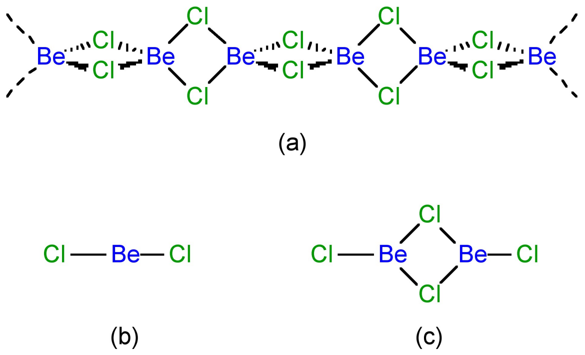

**Figure 4.44:** Structures of $BeCl_2$.

## 4.3.2 Magnesium

The ionic radius for the +2 cation of magnesium is fairly small (0.65 Å). As a consequence the charge density (z/r) is high, which results in a high polarizing power of the $Mg^{2+}$ ion. Thus, magnesium tends to form polar covalent bonds rather than ionic complexes. As with lithium there is a wide range of organometallic derivatives of magnesium, especially the Grignards (RMgX, where X = Cl, Br).

A further consequence of the covalent character of the bonding is that magnesium tends to form either 4-coordinate (tetrahedral) or 6-coordinate (octahedral) complexes with well-defined geometries.

# 4.4 Organometallic Compounds of Magnesium[9]

While beryllium makes a range of organometallic compounds, their hazardous nature has limited their study. In contrast, the ionic nature of calcium, strontium, and barium compounds limits the number of stable

---

[9] This content is available online at <http://cnx.org/content/m32494/1.2/>.

organometallic derivatives. However, the organometallic chemistry of magnesium is rich and extensive. The importance of Grignards (RMgX, where X = halide) and dialkyl magnesium compounds ($R_2Mg$) is due to their use in organic synthesis and as synthons for a range of organometallic compounds.

## 4.4.1 Grignard reagents

Grignard reagents (and the Grignard reaction using these compounds) are named after Victor Grignard (Figure 4.45). After studying mathematics at Lyon he transferred to chemistry, becoming a professor at the University of Nancy in 1910. During World War I, he was involved in the field of chemical warfare; however, it is for his major contribution to organic chemistry he is remembered.

**Figure 4.45:** French chemist and Nobel Prize winner François Auguste Victor Grignard (1871 – 1935).

### 4.4.1.1 Preparation

The general the synthesis of a Grignard reagent involves the reaction of an alkyl halide (RX, where X = Cl, Br, I) with magnesium metal in a suitable ether solvent, (4.24).

$$RX + Mg \rightarrow RMgX \tag{4.24}$$

While diethyl ether ($Et_2O$) and tetrahydrofuran (THF) are commonly used as solvents, other polar non-protic solvents are suitable, including: triethylamine ($NEt_3$), dimethylsulphide ($Me_2S$), dimethylselenide ($Me_2Se$), and dimethyltelluride ($Me_2Te$).

In general the alkyl halide is added to an excess of magnesium suspended in the solvent. In most cases it is necessary to activate the magnesium, by the addition of iodine ($I_2$), 1,2-dibromoethane, or sonication. If the halide is very inert reaction can be promoted by the co-condensation of magnesium and THF under vacuum.

There is often an induction period after the initial addition of alkyl halide. However, since the reaction, (4.24), is highly exothermic care should be taken to ensure that the reaction does not run-away. For this reason it is normal to initially add a small quantity of the alkyl halide to ensure the reaction initiates. Once reaction is initiated, the addition of alkyl halide is maintained at a suitable rate to ensure the reaction is maintained until all the alkyl halide is consumed. The excess reaction magnesium is removed from the reaction mixture by filtration.

It is not always necessary to use a liquid or solid halide dissolved in the solvent. Bubbling methyl chloride (MeCl) through an $Et_2O$ suspension of magnesium yields MeMgCl. The advantage of a gaseous alkyl halide is that the reaction is very clean as all the magnesium is consumed and the excess alkyl halide is bubbled away.

The purity of the magnesium is very important. For his original experiments Grignard used magnesium of a purity of 99.2%. However, it is now more typical to use 99.8% pure magnesium. It is important that the magnesium not be too pure since it is thought that the transition metal impurities catalyze the reaction.

The relative order of reactivity of the alkyl halide follows the trend:

$$\mathrm{I > Br > Cl > F} \qquad (4.25)$$

In fact alkyl fluorides are sufficiently inert that highly coordinating polar solvents such as THF or dimethylformamide (DMF) must be used.

If the reaction is allowed to get too hot then several possible side reactions can occur. In THF reaction with the solvent occurs:

$$\mathrm{RMgX + THF \rightarrow RH + H_2C{=}CH_2 + H_2C{=}C(H)MgX} \qquad (4.26)$$

Alternatively, a transition metal catalyzed radical coupling between the Grignard and unreacted alkyl halide is observed irrespective of the identity of the solvent, (4.27).

$$\mathrm{RMgX + RX \rightarrow R\text{-}R + MgX_2} \qquad (4.27)$$

The mechanism for Grignard formation is thought to be radical in nature; however, a study of the surface of the magnesium during the reaction has shown the presence of corrosion pits. It is generally agreed that initiation occurs at surface dislocations, but the major reaction occurs at a polished surface.

The kinetics of the reaction is 1st order with respect to the alkyl halide concentration, but it has also been claimed to be 1st order with respect to the solvent concentration. It has therefore been concluded that the rate-determining step involves the metal solvent interface.

The reaction of magnesium with aryl bromides has been studied and is proposed to occur by two reactions. The first involves electron transfer between the aryl halide and the metal, while the second involves aryl radical formation.

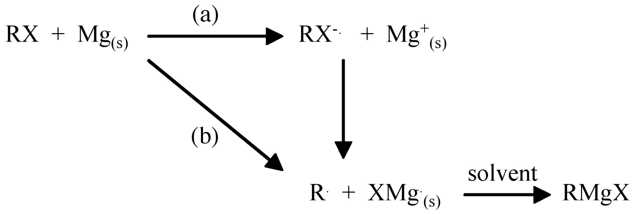

(4.28)

A number of alternative synthetic routes are used with polyhalogenated hydrocarbons, (4.29) and (4.30), and where the alkyl radical is unstable, (4.31).

$$\mathrm{X_3CH + {}^iPrMgX \rightarrow (X_3C)MgX + {}^iPrH} \qquad (4.29)$$

$$\mathrm{C_6Br_6 + EtMgX \rightarrow (C_6Br_5)MgX + EtBr} \qquad (4.30)$$

$$\mathrm{RX + R'MgX' \rightarrow RMgX' + R'X} \qquad (4.31)$$

#### 4.4.1.2 Structure

The solid state structure of Grignard reagents is controlled by the presence and identity of the solvent used in the synthesis. In this regard the size and the basicity of the solvent is important. For example, the structure of EtMgBr crystallized from diethyl ether exists as a 4-ccordinate monomer (Figure 4.46a), while the use of the sterically less demanding THF results in a 5-coordinate monomeric structure (Figure 4.46b). In contrast, the use of triethylamine yields a dimeric bromide bridged structure (Figure 4.46c), and the use of a chelate bidentate amine gives a structure (Figure 4.46d) similar to that observed with diethyl ether (Figure 4.46a).

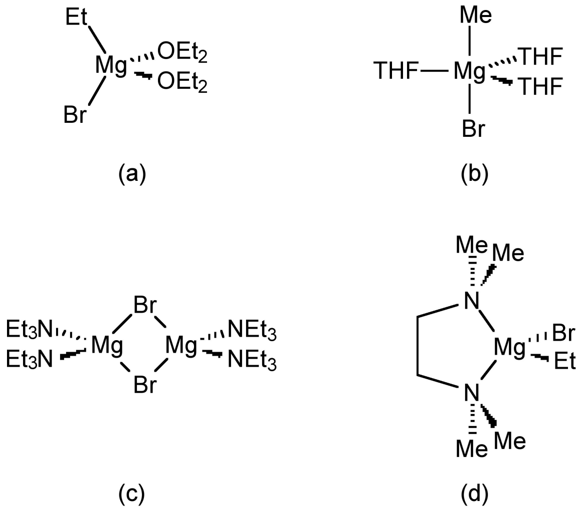

**Figure 4.46:** Molecular structure of EtMgBr in (a) diethyl ether, (b) THF, (c) triethyl amine, and (d) tetramethyletheylenediamine (TMED).

In solution, Grignards are fluxional such that no single defined structure is present. The series of exchange reactions are known as an extended Schlenk equilibrium (Figure 4.47).

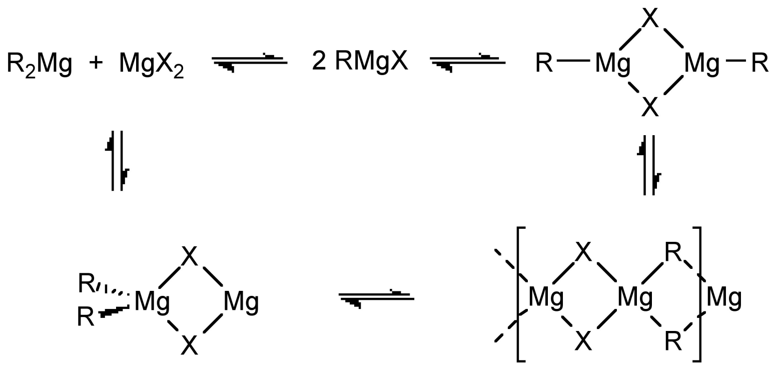

**Figure 4.47:** Schematic representation of the extended Schlenk equilibrium observed for Grignard compounds in solution.

It is observed that Grignard solutions are also slightly conducting, and magnesium is deposited at both the anode and cathode suggesting the formation of $RMg^+$ and $[RMgX_2]^-$. The alkyl/halide exchange is thought to occur through a bridging intermediate (Figure 4.48).

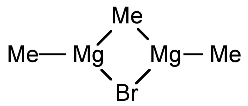

**Figure 4.48:** Proposed structure for the alkyl/halide exchange bridging intermediate.

## 4.4.2 Dialkyl magnesium ($R_2Mg$)

Dialkyl magnesium compounds are involatile white solids. They generally have similar reactivity to their Grignard analogs.

### 4.4.2.1 Synthesis

The most common synthesis of $R_2Mg$ is by the reaction of a Grignard with dioxane ($C_4H_8O_2$), (4.32), where the precipitation of the dihalide is the reaction driving force.

(4.32)

This method is useful for the synthesis of cyclic compounds, (4.33).

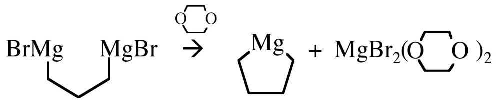

(4.33)

An alternative synthesis that does not require dioxane involves the metal exchange reaction between magnesium metal and a dialkyl mercury compound.

$$R_2Hg + Mg \rightarrow R_2Mg + Hg \tag{4.34}$$

Finally, in selected cases, magnesium will react with acidic hydrocarbons such as cyclopentadienyl at high temperatures (600 °C).

### 4.4.2.2 Structure

In the vapor phase dialkyl magnesium compounds are generally monomeric linear compounds. In solution, in the absence of coordinating solvents $R_2Mg$ form a variety of oligomers (Figure 4.49a-c) in solution as determined by molecular weight measurements. In the presence of coordinating solvents 4-coordinate monomers predominate (Figure 4.49d).

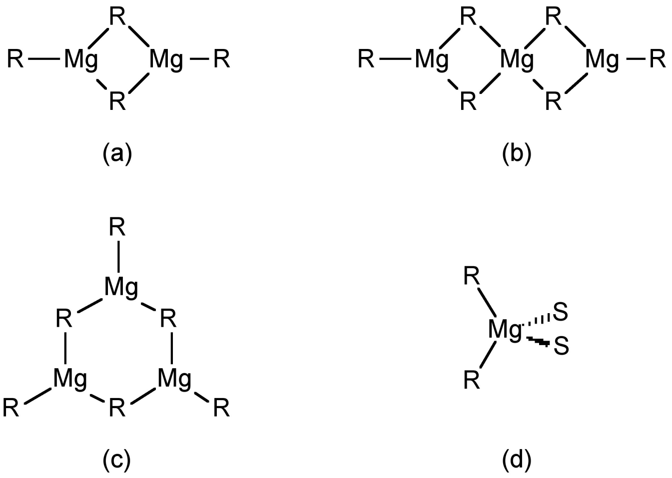

**Figure 4.49:** Solution structure of $R_2Mg$ (R = Me, Et) in (a – c) non-coordinating solvents, and (d) diethyl ether.

As similar trend is observed in the solid state, where polymers have been characterized in the absence of coordinating solvents (Figure 4.50a), while monomers or dimmers are generally observed when crystallized from a coordinating solvent (Figure 4.50b and c).

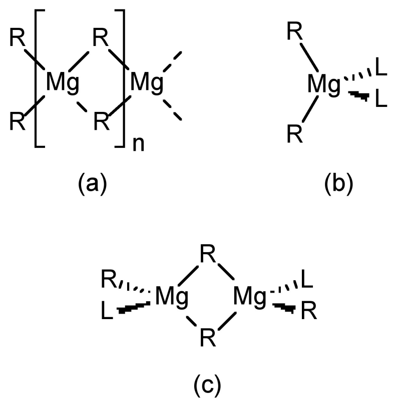

**Figure 4.50:** Solid state structure of $R_2Mg$ (R = Me, Et) crystallized in (a) the absence and (b and c) the presence of a coordinating solvents.

## 4.4.3 The use of organomagnesium compounds in organic synthesis

### 4.4.3.1 Hydrolysis and related reactions

Grignard compounds react with water to give the hydrocarbon, (4.35), they also react with other hydroxylic compounds such as alcohols and carboxylic acids. One important use of the hydrolysis reaction is specifically deuteration, (4.36).

$$CH_3MgBr + H_2O \rightarrow CH_4 + BrMgOH \tag{4.35}$$

$$CH_3CH_2(CH_3)_2CMgBr + D_2O \rightarrow CH_3CH_2(CH_3)_2CD + BrMgOD \tag{4.36}$$

The hydrogen atom on a terminal alkyne is sufficiently acidic that the reaction with Grignards occurs in an analogous manner to that of hydrolysis.

$$C_6H_5C{\equiv}CH + C_2H_5MgBr \rightarrow C_6H_5C{\equiv}CMgBr + C_2H_6 \tag{4.37}$$

Once formed the alkynyl Grignard undergoes the same hydrolysis reaction.

$$C_6H_5C{\equiv}CMgBr + D_2O \rightarrow C_6H_5C{\equiv}CD + BrMgOD \tag{4.38}$$

### 4.4.3.2 Reaction with $CO_2$

Grignards react readily with carbon dioxide to form the carboxylate, which yields the associated carboxylic acid upon hydrolysis, (4.39).

$$RMgX + CO_2 \rightarrow RCO_2MgX \xrightarrow{H_2O} RCO_2H + HOMgX \tag{4.39}$$

### 4.4.3.3 Reaction with carbonyls

Organomagnesium compounds react with organic carbonyls (aldehydes, ketones, and esters) to yield the alcohol on hydrolysis, (4.40). This synthetic route is useful for the formation of primary, secondary and terminal alcohols.

$$RMgX + R'_2C{=}O \rightarrow R'_2(R)COMgX \xrightarrow{H_2O} R'_2(R)COH + HOMgX \qquad (4.40)$$

Unfortunately, for some carbonyls there is a competing side reaction of enolization, where the starting ketone is reformed upon hydrolysis.

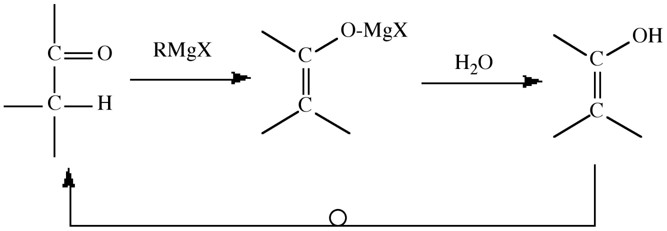

(4.41)

When the Grignard reagent has a $\beta$-hydrogen another side reaction occurs in which the carbonyl group is reduced and an alkene is formed.

$$R_2C{=}O + (CH_3CH_2)MgX \rightarrow R_2(H)COH + H_2C{=}CH_2 \qquad (4.42)$$

Both the enolization and reduction occur via similar 6-membered cyclic transition states (Figure 4.51).

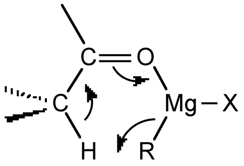

**Figure 4.51:** Representation of the 6-membered transition state reaction for enolization of a ketone.

Grignards react with $\alpha$,$\beta$-unsaturated ketones to give either the 1,2-addition product or the 1,4-addition product, or both.

$$Ph(H)C{=}C(H)\text{-}C(O)Me + EtMgBr \xrightarrow{H_2O} \begin{array}{c} Ph(H)C{=}C(H)\text{-}C(OH)EtMe \\ + \\ Ph(H)EtC\text{-}CH_2\text{-}C(O)Me \end{array} \qquad (4.43)$$

### 4.4.3.4 Reaction with acyl halides

Acyl halides react with Grignards to give ketones, (4.44). Best results are obtained if the reaction is carried out at low temperature and in the presence of a Lewis acid catalysts (e.g., $FeCl_3$).

$$CH_3C(O)Cl + RMgX \rightarrow CH_3C(O)R + XMgCl \qquad (4.44)$$

#### 4.4.3.5 Reaction with epoxides

Oxirane (epoxide) rings are opened by Grignards, (4.45), in a useful reaction that extends the carbon chain of the Grignard by two carbon atoms. This reaction is best performed with ethylene oxide since the magnesium halide formed is a Lewis acid catalyst for further reactions in the case of substituted oxiranes.

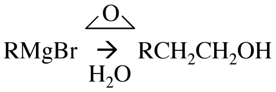

$$\mathrm{RMgBr} \xrightarrow[\mathrm{H_2O}]{\mathrm{O}} \mathrm{RCH_2CH_2OH} \tag{4.45}$$

#### 4.4.3.6 Reaction with salts

One of the most useful methods of preparing organometallic compounds is the exchange reaction of one organometallic compound with a salt of a different metal, (4.46). This is an equilibrium process, whose equilibrium constant is defined by the reduction potential of both metals. In general the reaction will proceed so that the more electropositive metal will form the more ionic salt (usually chloride).

$$\mathrm{RM + M'X \rightleftharpoons RM' + MX} \tag{4.46}$$

Grignard reagents are particularly useful in this regard, and may be used to prepare a wide range of organometallic compounds. For example:

$$\mathrm{2\,CH_3CH_2MgCl + CdCl_2 \rightarrow Cd(CH_2CH_3)_2 + 2\,MgCl_2} \tag{4.47}$$

$$\mathrm{4\,CH_3MgCl + SiCl_4 \rightarrow Si(CH_3)_4 + 4\,MgCl_2} \tag{4.48}$$

The reaction with a Grignard is milder than the analogous reaction with lithium reagents, and leads to a lower incident of side-products.

## 4.4.4 Bibliography

- H. Bader and N. M. Smyth, *J. Org. Chem.*, 1964, **29**, 953.
- C. L. Hill, J. B. Vander Sande, G. M. Whitesides, *J. Org. Chem.*, 1980, **45**, 1020.
- E. Weiss, *J. Organomet. Chem.*, 1964, **2**, 314.
- A. R. Barron, *J. Chem. Soc., Dalton Trans.*, 1989, 1625.